Continental Shelf Research 70 (2013) 74–87

Contents lists available at ScienceDirect

Continental Shelf Research

journal homepage: www.elsevier.com/locate/csr

Research papers

Plankton and seston size spectra estimated by the LOPC and ZooScan in the Abrolhos Bank ecosystem (SE Atlantic)

Catarina da Rocha Marcolin [a,*], Sabine Schultes [a,1], George A. Jackson [b], Rubens M. Lopes [a]

[a] Oceanographic Institute, University of São Paulo, Praça do Oceanográfico, 191, Sala 100, 05508-120 São Paulo, SP, Brazil
[b] Department of Oceanography, Texas A&M University, Eller O&M Building 3146 TAMU, College Station, TX 77843-3146, USA

ARTICLE INFO

Available online 27 September 2013

Keywords:
Mesozooplankton
Particles
Coral reefs
Vertical distribution
Spatial variation
NBSS

ABSTRACT

The biomass size spectrum provides valuable information about the functioning of plankton systems. We evaluated hydrographic and bathymetric influences on biomass size spectra and on vertical distributions of plankton and seston above the Abrolhos Bank and in adjacent oceanic areas off Eastern Brazil. We used both *in situ* Laser Optical Particle Counter (LOPC) and preserved plankton samples analyzed with a ZooScan system to determine seston and plankton abundances, size distributions, and biomasses. Shelf stations, including those on the Abrolhos Bank, had higher particle concentrations and mesozooplankton biomasses than the vertically stratified oceanic stations. The latter were influenced by cold, nutrient-rich South Atlantic Central Water (SACW) below the mixed layer, particularly toward the south of the study area. Small particles (<1 mm) were more abundant above and within the pycnocline, whereas large particles (>1 mm) had a more heterogeneous vertical distribution, but were more abundant above the pycnocline, especially at the oceanic stations. Calanoid copepods usually dominated the mesozooplankton biomass spectra, but were accompanied by cyclopoids, appendicularians, and ostracods, the latter being particularly abundant during nighttime stations on the Abrolhos Bank. Both LOPC and ZooScan data showed significant differences in NBSS slopes and intercepts between shelf and oceanic stations. The higher intercepts and steeper slopes over the shelf are characteristic of higher productivity. The shallower slopes and presence of more biomass in larger particles indicate a more important contribution of large organisms and higher energy transfer efficiencies at the open ocean stations. Our results highlight the importance of the Abrolhos Bank for pelagic production in an otherwise oligotrophic ocean.

1. Introduction

Since the pioneering work of Sheldon et al. (1972), plankton systems have often been described on the basis of organism size and biomass spectra, as these estimates provide useful information about ecosystem structure (Quinones, 1994), and have the potential to reveal ecological interactions not so easily depicted with conventional taxonomic approaches (Krupica et al., 2012). The theory of the Normalized Biomass Size Spectrum (NBSS; Kerr and Dickie, 2001) associates the intercepts and slopes of a linear regression fitted to the spectrum with biomass production rates, energy transfer efficiencies and predator–prey interactions (Zhou, 2006). The NBSS and other size-based indices have been used in theoretical models to explore coupling between predator and detritivore communities (Stock et al., 2008; Blanchard et al., 2009). Empirical methods have used the NBSS to estimate population dynamics parameters (Zhou and Huntley, 1997), to evaluate the effects of nutrient enrichment in estuaries (Moore and Suthers, 2006), to determine the effects of fisheries on coral reefs (Graham et al., 2005), to detect spatial and temporal trends in plankton communities (Krupica et al., 2012), and to describe size-structured food webs (Jennings and Mackinson, 2003).

Marine ecosystem structure is tightly connected to both bottom-up and top-down control mechanisms that have consequences for organism size structure (Gilabert, 2001; Suthers et al., 2006). Hydrographic features, such as presence of a pycnocline or nutrient input from deep waters or estuaries, are typical examples of physical features providing bottom-up control. The effects of such processes should be observable on zooplankton biomass size spectra. For instance, Finlay et al. (2007) found that bottom-up effects were strong drivers of zooplankton size structure in lakes.

With the development of optical instrumentation having the capability for high-quality image acquisition or particle counting and sizing, plankton size and biomass can now be more quickly estimated both *in situ* and in the laboratory (Benfield et al., 2007; Stemmann and Boss, 2012). One example is the Laser Optical Particle Counter, which generates higher size-resolved information on particle abundance – detecting particles over the size range of 100 μm–35 mm reported

* Corresponding author. Tel.: +55 11 3091 6556; fax: +55 11 3091 6607.
E-mail addresses: catmarcolin@gmail.com (C.R. Marcolin), schultes@biologie.uni-muenchen.de (S. Schultes), gjackson@tamu.edu (G.A. Jackson), rubens@usp.br (R.M. Lopes).
[1] Present address: LMU Munich, Department of Ecology, Munich, Germany.

0278-4343/$ - see front matter © 2013 Elsevier Ltd. All rights reserved.
http://dx.doi.org/10.1016/j.csr.2013.09.022

Equivalent Spherical Diameter (ESD) – than its previous generation, the OPC, which detected particles over a size range of ~250 μm–25 mm (Herman et al., 2004). Recently developed analytical tools have provided means to distinguish large zooplankton (>1 mm) from marine snow for LOPC data using particle opacity and size (Checkley et al., 2008; Jackson and Checkley, 2011). Optical measurements may, therefore, deliver continuous *in situ* data of particle distributions with more accuracy, resolution, and regularity than previous methods (Boyd and Trull, 2007; Guidi et al., 2008).

The data from particle counters and *in situ* imaging devices can be compared with zooplankton abundance and biomass measurements obtained from plankton tows (Herman and Harvey, 2006; González-Quirós and Checkley, 2006; Schultes and Lopes, 2009; Schultes et al., 2013). Image analysis of net samples provides a quick way to obtain size and biomass distributions of zooplankton. For example, the benchtop ZooScan can generate plankton size distributions for a large number of preserved samples (Gorsky et al., 2010). Schultes and Lopes (2009) found that the comparison between LOPC and scanned net samples can be difficult in shallow waters over the Abrolhos Bank due to high detrital particle loads there. This is expected because the LOPC is not able to distinguish between detritus and organisms, particularly for objects smaller than 2 mm, and because of the different responses to detritus of the two sampling methods.

Differences between the LOPC tunnel area and the mouth of the net lead to sampling biases (Schultes and Lopes, 2009). For example, large organisms can avoid the LOPC tunnel, but not the net opening, and small organisms and fragile particles can be detected by the LOPC, but are not retained by the nets. Despite these differences, the size structure, *i.e.* NBSS, is a conservative and informative characteristic of planktonic communities that is independent of taxonomy (Kerr and Dickie, 2001). Studies including size spectra from both LOPC and net plankton estimates with image analysis are rare in the literature (*e.g.* Schultes and Lopes, 2009; Schultes et al., 2013). We will test if LOPC and ZooScan NBSS parameters are comparable, providing the same responses to different environments. If they do, the LOPC can provide a valuable monitoring tool because of its ability to generate a large amount of interpretable data very quickly.

The Abrolhos Bank is the largest extension of the narrow Eastern Brazilian continental shelf, extending up to 220 km into the ocean. The bank harbors the world's largest contiguous rhodolith bed, covering about 20,900 km^2 (Amado-Filho et al., 2012), is the largest coral reef system of the South Atlantic, and supports an exceptionally high biodiversity (Leão, 1996; Werner et al., 2000). South of Abrolhos Bank, seamounts are found along the Vitória-Trindade Ridge. The productive waters of the bank exert a profound influence on the economic and social dynamics of the area, especially on fishing and tourism (Costa et al., 2003).

The plankton community structure of the Abrolhos Bank and vicinity is poorly known. Previous studies have provided descriptions of the composition, abundance, and biomass distribution of both phyto- and zooplankton (Valentin et al., 1993; Brandini et al., 1997; Ekau, 1999; Knoppers et al., 1999; Susini-Ribeiro, 1999), as well as on phytoplankton production (Gaeta et al., 1999), but no information on plankton size structure is available. In fact, plankton communities are often neglected in coral reef studies worldwide, although they represent a significant food source for reef-building corals (Porter, 1976; Ferrier-Pagès et al., 2003) and associated biota, especially reef fish (Russell, 1983).

In this paper, we evaluate hydrographical and bathymetric influences on the plankton composition and size spectra of the Abrolhos Bank and adjacent oceanic areas using a combination of *in situ* and laboratory-based approaches to determine seston and plankton abundance and biomass. We hypothesize that shelf and oceanic areas have contrasting plankton and particle size structures, and use NBSS intercepts and slopes as our working tools. We also test for differences between shelf and oceanic stations with respect to their mesozooplankton and particle biomass.

2. Material and methods

2.1. The study region

The observations were made during the PROABROLHOS winter expedition, conducted off the coast of Brazil in July–August 2007

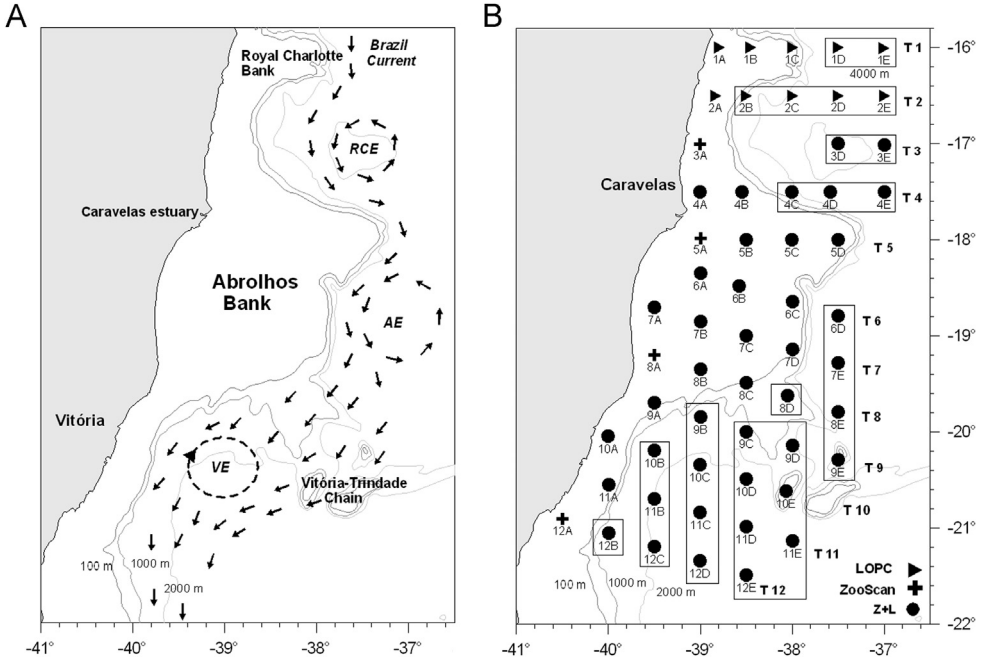

Fig. 1. Station map showing the location of the Abrolhos Bank and a simplified scheme of the currents in the region ((A), see also Soutelino et al., 2013) and the location of LOPC, ZooScan, and both LOPC and ZooScan (L+Z) stations (B). RCE: Royal Charlotte Eddy; AE: Abrolhos Eddy; VE: Vitória Eddy. The boxes in B indicate oceanic stations. Abrolhos Bank and vicinities; July–August 2007. All subsequent figures refer to the same sampling area and period.

(Fig. 1). Sampling covered oceanographic settings ranging from shallow, turbid, near-shore waters to oligotrophic "blue waters" over the continental slope during day or night. Stations were categorized as either "shelf" or "oceanic" (see Fig. 1, oceanic stations inside boxes), based on the distance from the coast and the local depth (shelf: from 19 m—station 1A to 78 m—station 8C; oceanic from 474 m—station 3E to 4032 m—station 1E). There was a total of 56 stations, with 51 sampled using the LOPC and 46 sampled with plankton nets.

2.2. LOPC and zooplankton sampling

The LOPC was the main sampling tool of this study. An LOPC660 model with a size detection range of 0.1–35 mm was installed inside a conical-cylindrical, 200-μm mesh-sized ring net (diameter 60 cm) with an interoperable Micro-CTD (AML Microsystems). A calibrated flowmeter (General Oceanics; Mechanical Digital Flowmeter Model 2030) was installed on the T-frame where LOPC was mounted, outside the LOPC tunnel and within the net ring, in accord with the LOPC user manual. This apparatus was towed as close to the bottom as possible, but no deeper than ~200 m. Average LOPC tow speed was 0.77 m s^{-1} ($\pm$0.13 std).

The net samples were recovered immediately and fixed in formaldehyde (4% final concentration) buffered with sodium tetraborate for subsequent scanning and image analysis. Further details on LOPC sampling are presented in Schultes and Lopes (2009). Fluorescence was estimated with a fluorometer, which was deployed coupled to a CTD (Falmouth Scientific Inc.). The Brunt–Väisälä frequency (BV) distributions were calculated from salinity, temperature and depth profiles using the Matlab™ seawater toolbox (Morgan, 1994). The BV frequency is proportional to the square root of the density gradient and is often used as a measure of seawater density stratification.

2.3. Plankton processing with the ZooScan

Preserved zooplankton samples were scanned with the ZooScan system (Grosjean et al., 2004) at a resolution of 2400 dpi, following the scanning protocol described in Schultes and Lopes (2009). A fraction of each plankton sample (1/8–1/128) was isolated with a Motoda splitter and analyzed after being scanned in duplicate. Images were processed with *Zooprocess*. The lower recognition size limit of particles was set to 250 μm reported equivalent spherical diameter (ESD).

The *Zooprocess* software isolates images, known as vignettes, of individual objects. For each vignette, a range of parameters relating to size, grey level and form were stored in a result file (*.pid), which was subsequently loaded into *Plankton Identifier* (Gorsky et al., 2010). Vignettes were classified using the Random Forest algorithm in *Plankton Identifier* (Version 1.3.0). Cross validation of the learning set yielded variable recall values, *e.g.* 0.93 (*Cyclopoida*), 0.88 (*Appendicularia*), 0.86 (*Thaliacea*), 0.85 (*Ostracoda*), 0.77 (*Chaetognatha*), 0.73 (*Calanoida*), 0.72 (*Poecilostomatoida*), and 0.45 (detritus, such as: sand/silt, aggregates, exuvia, fecal pellets and undetermined organic debris). Results were then manually validated to correct for residual misclassification among the taxonomic categories presented in here. The validated results were processed to remove noise, inorganic fibers, scanning artifacts, and vignettes with multiple organisms. Typically, there were fewer than 5% of the vignettes with multiple organisms for a sample.

Biomass was estimated for each organism from its volume, assuming that all were shaped as prolate spheroids with an axis ratio of 3:1 and a density of 1 mg mm^{-3}. Normalized Biomass Size Spectra (NBSS) were then calculated by summing the accumulated biomass as a function of size for the size bins provided by the LOPC post-processing software (Schultes and Lopes, 2009). The slopes and intercepts were calculated by fitting a linear regression to each spectrum using log-transformed data. The values for the lower and upper size ranges of each spectrum were removed to compensate for the low sampling efficiency of the net at these boundaries. Hopcroft et al. (2001) estimated that a 200-μm net is more efficient for sampling organisms from 450 to 1400 μm prosome length in tropical regions. Taking that into account, we included only size classes ranging from the peak of the distribution up to the first empty class for the calculation of NBSS slopes and intercepts.

2.4. LOPC calculations of NBSS distributions

The LOPC and the AML Micro-CTD data were processed with the LOPC post-processing routine using the exact sample counts (LOPC_PostPro, available at www.alexherman.com) to obtain data with a vertical resolution of 1 m, cutting-off the upper 2 m depth to minimize false counts of air bubbles near the surface. We calculated the log normalized biomass size spectra (NBSS) for each sample as $NBSS = \Delta M/\Delta m$, where ΔM is the total particle mass in a size region and Δm is the difference in mass of the largest and smallest possible particles for that region. The slopes and intercepts were calculated by fitting a linear regression to each spectrum. The same criteria were used to calculate NBSS slopes and intercepts for LOPC samples as for those from ZooScan. Data was adjusted for differences in sampling volume between LOPC and ZooScan.

2.5. Data treatment and statistical analysis

After checking for the normality and homoscedasticity of the NBSS parameters, Wilcoxon or Student's *t*-test were used to test for differences in NBSS slopes and intercepts, calculated with both LOPC and ZooScan, according to the station categories. All tests were performed using the package "pgirmess" in the statistical environment R (R Development Core Team, 2011; Giraudoux, 2012). For data manipulation and plotting we used "lattice" (Sarkar, 2008) and "gtools" (Warnes, 2013).

The volume spectrum (*nVd*, where *n* is the number spectrum, *V* is particle volume, and *d* is diameter) describes the distribution of particle volume normalized so that the area under a curve is proportional to the integrated particle volume when plotted against the logarithm of the particle diameter (ESD). We computed it as in Checkley et al. (2008). We calculated the vertically integrated total particle volume per unit area ($cm^3\ m^{-2}$) after first determining the total particle concentration per volume through the water column ($cm^3\ m^{-3}$) by integrating *nVd* with respect to log of diameter; we then integrated the result with respect to depth. We used this vertically-integrated particle volume to describe spatial differences between shelf and oceanic stations. We dropped samples from the 0–2 m depth range to minimize false counts of gas bubbles. We also checked this total particle volume distribution for normality and homoscedasticity; total volume values were log-transformed to achieve a normal distribution and a Student *t*-test was used to test differences between station categories.

Although previous authors have been able to distinguish marine snow from LOPC data using particle opacity characteristics (Checkley et al., 2008; Jackson and Checkley, 2011), we did not have enough samples to perform this analysis with statistical accuracy.

3. Results

3.1. Environmental variables

Temperature and salinity were both vertically homogeneous through the water column in the shelf stations, while in the oceanic

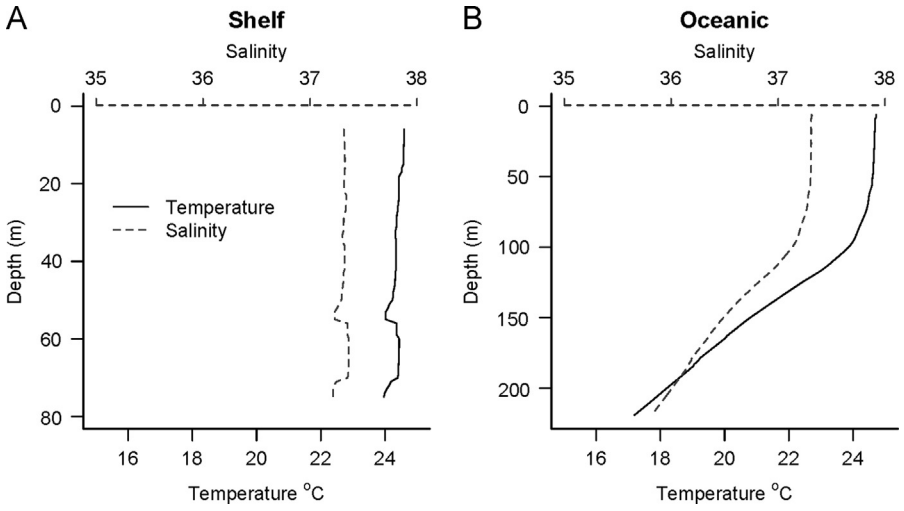

Fig. 2. Vertical profiles of temperature °C and salinity, averaged for shelf (A) and oceanic (B) stations, as defined in the text. Note the different scales for the depth axes.

Table 1
Descriptive statistics of environmental variables and Normalized Biomass Size Spectra (NBSS) parameters in the Shelf and Oceanic Stations. Abrolhos Bank and vicinities. July–August 2007.

	Shelf		Oceanic	
	Mean ± std	Range	Mean ± std	Range
Temperature	24.48 ± 0.61	22.12 25.81	23.20 ± 2.23	15.51–26.02
Salinity	37.32 ± 0.22	36.54–37.66	35.93 ± 0.95	34.50–37.61
BV	$1.9 \times 10^{-5} \pm 6.5 \times 10^{-5}$	$-1.3 \times 10^{-4} - 1.1 \times 10^{-3}$	$4.1 \times 10^{-5} \pm 5.0 \times 10^{-5}$	$-7.4 \times 10^{-5} - 4.8 \times 10^{-4}$
Fluorescence	0.42 ± 0.15	0.12–0.95	0.14 ± 0.08	0.01–0.55
NBSS				
Intercept LOPC	4.81 ± 0.49	3.86–5.62	3.76 ± 0.26	3.41–4.23
Intercept ZooScan	4.36 ± 0.43	3.72–5.61	3.58 ± 0.37	2.91–4.21
Slope LOPC	−0.96 ± 0.15	−1.25/−0.74	−0.86 ± 0.06	−0.95/−0.75
Slope ZooScan	−1.01 ± 0.20	−1.40/−0.67	−0.91 ± 0.19	−1.41/−0.61

stations, it sharply decreased below ~100 m (Fig. 2). The average temperature was higher at shelf than oceanic stations (Table 1) because of the greater tow depths (up to 200 m) at oceanic stations, which included colder deep water. Higher values of the BV frequency distribution were found at the oceanic stations than at the shelf, a result of the stratification of the water column offshore. Mean fluorescence was significantly higher ($p<0.01$) on the shelf, with highest values above the Abrolhos Bank, at stations 4B (mean=0.79), 4A (mean=0.57) and 5B (mean=0.59).

3.2. Particle and mesozooplankton spatial distribution

The shelf stations had significantly greater ($p=0.05$) total particle volumes (108.2 ± 75.6 cm^3 m^{-2}) than oceanic stations (70.4 ± 74.3 cm^3 m^{-2}; Fig. 3A; LOPC data). There appeared to be a north-south gradient in the shelf total particle volume, with higher values on the Abrolhos Bank than at the southernmost coastal stations. Larger particles (>1 mm) dominated biomass at the southernmost shelf stations (from station 6A on), in the region where the oceanic influence is greater (Fig. 3A), as well as at the oceanic stations. Mesozooplankton biomass was greater at the shelf stations, both on the Abrolhos Bank and at the southernmost region, particularly during nighttime observations (Fig. 3B; ZooScan data). Diel variations were not as evident for total particle volume estimates. Mean mesozooplankton biomass over the shelf ranged from 3.1 to 591.9 mg m^{-3} (mean=162.9 ± 139.5 mg m^{-3}), while mean biomass at the oceanic stations ranged lower, from 1.2 to 219.2 mg m^{-3} (mean=57.3 ± 56.3 mg m^{-3}). Mesozooplankton biomass per unit area was also significantly greater ($p<0.01$) over the shelf than offshore. Calanoids were the dominant group at the majority of stations (Fig. 3C). However, the highest biomass values were at stations 7C and 8B (above the Abrolhos Bank) and were associated with high concentrations of ostracods during nighttime. Ostracods were as much as 72% of the total biomass there. Appendicularians were abundant at some of the stations furthest from the coast and those above seamounts (3D and 10E). The dominance of calanoids was striking on the shelf, while the oceanic stations also included important contributions in all size classes from other groups, especially the cyclopoids (see Section 3.4).

In the southernmost stations, large organisms such as salps and chaetognaths were the main contributors to the biomass of the system, leading to high total biomass values there (Fig. 4). Because of their large sizes, these organisms were important contributors to total biomass even when at low numerical abundances (*e.g.* stations 7B, 7C, 8B, 10C and 11A).

Vertical profiles at shelf stations (Fig. 5) show two general patterns: (i) small particles had greater biomass than large particles at 71% of the stations; exceptions were 6 (1BC, 5D, 6BC, 8C) out of 21 stations; (ii) particles were, in general, homogenously distributed throughout the water column. Small particles increased slightly towards the bottom. This was the case at 8 out of 21 stations, *i.e.* 38%. These stations were 1A, 2A, 4A, 5C, 6A, 7AB, 8B, which are mostly coastal and very shallow. Resuspension of sediment there could explain this increase. Profiles obtained at three offshore stations over seamounts (3D, 8D, 10E) are presented separately in Fig. 5 and show no obvious tendency.

Vertical profiles at oceanic stations (Fig. 6) show three general patterns: (i) small and large particles were equally important in terms of biomass; (ii) small particles decreased below the mixed layer at 19 out of 28 stations, *i.e.* 68%, except for stations 1E, 7E,

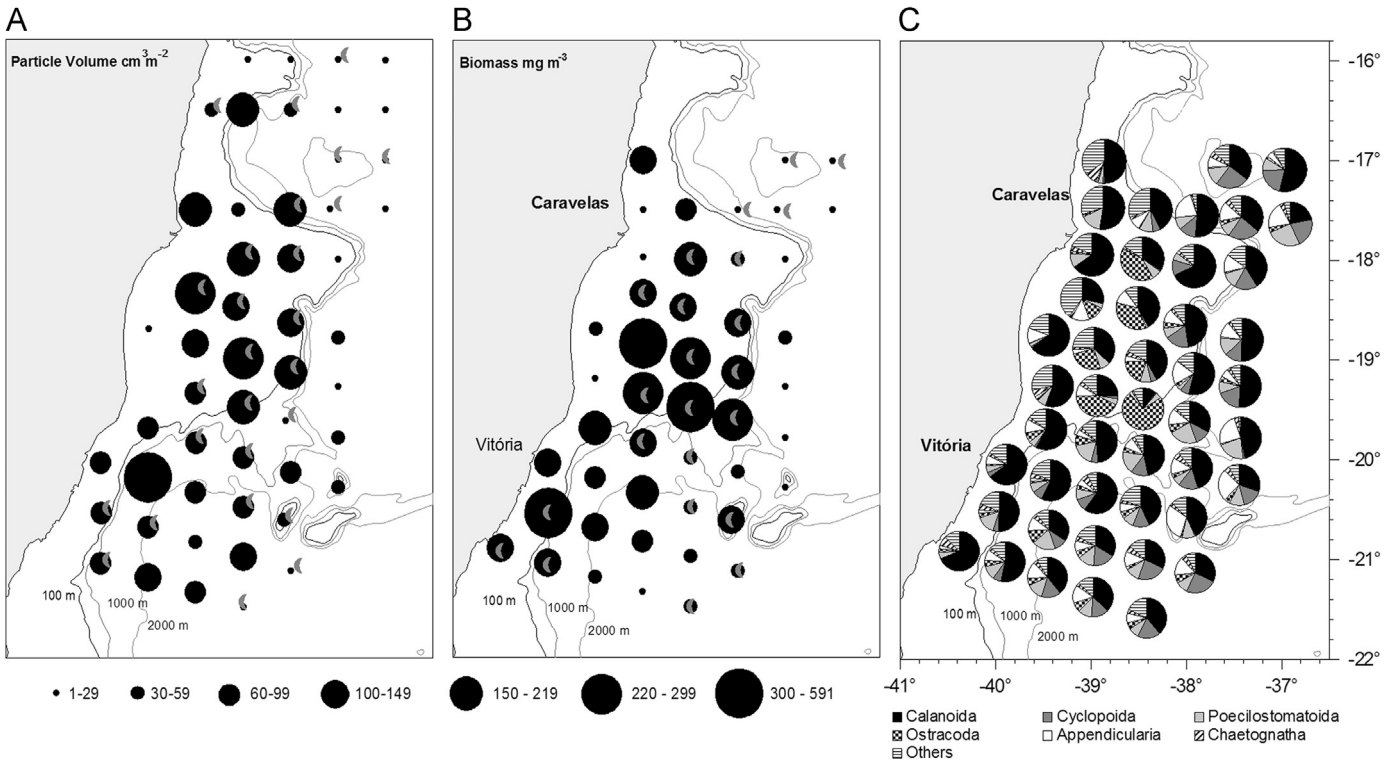

Fig. 3. Spatial distribution of total particle volume per unit area from LOPC data ($cm^3\ m^{-2}$) (A), mesozooplankton total biomass estimated using the ZooScan ($mg\ m^{-3}$) (B), and relative contribution (%) of the main mesozooplankton taxa to total biomass (C). Stations with "grey moon" symbols were sampled during the night.

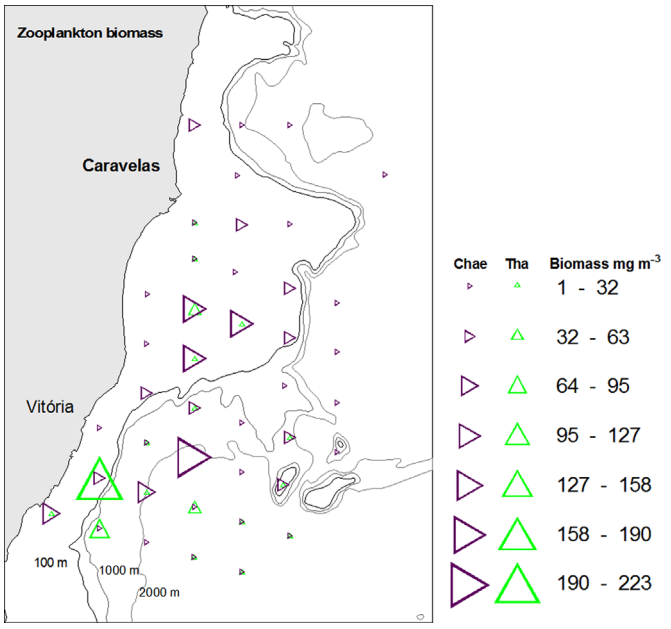

Fig. 4. Spatial distribution of biomass for chaetognaths (purple triangles) and thaliaceans (green triangles) estimated using the ZooScan ($mg\ m^{-3}$). (For interpretation of the references to color in this figure legend, the reader is referred to the web version of this article.)

9CD, 11CE, 12BCD most of which are situated in the area southeast of Abrolhos Bank; (iii) large particles had higher biomass in the mixed layer than below the thermocline at 22 out of 28 stations, *i.e.* 79%. Exceptions (1DE, 2BC, 3E, 10C) were mostly located to the north of Abrolhos Bank. Note that most of particle biomass vertical distributions were in phase with, or above, fluorescence and BV frequency peaks, especially for <1 mm particles.

The average of the vertical *nVd* size distribution is shown in Figs. 7 and 8. The mixed layer (as shown by the small values of the BV frequency), extended to the bottom of the sampling ranges over the shelf. Phytoplankton concentrations, as described by fluorescence, were high, especially above the Abrolhos Bank (Fig. 5), with largest values in the 15–30 m depth range (Fig. 7). The average particle maximum determined with the LOPC *nVd* distribution occurred between 10 and 30 m; particles ranging from approximately 0.35 to 1.0 mm were the main contributors to total particle volume. Large (>1 mm) particles were sporadically distributed in the water column.

At oceanic stations the thermocline depth varied widely from 50 m to more than 100 m (Fig. 6). Fluorescence was lower in the mixed layer close to the surface, increasing at 40–130 m depth; it did peak above the pycnocline, decreasing with depth (Fig. 8). Particles <1 mm were most abundant between 15 and 60 m depth, and were less abundant than over the shelf (Figs. 7 and 8). Particles >1 mm were present primarily in the upper 80 m and accounted for a large fraction of the total particle volume. Despite the greater numeric abundance of smaller-sized particles, larger particles were an important component of total particle biomass at the oceanic stations. The vertical distribution of particles <1 mm was associated with both BV and fluorescence distributions, with higher concentrations above the pycnocline and in regions where fluorescence was higher.

3.3. NBSS in relation to the distance from the coast

The shapes and parameters of the NBSS calculated from data collected by both LOPC and ZooScan were different at shelf and oceanic stations (Figs. 9 and 10). Shelf stations had significantly larger intercepts (LOPC: $p<0.01$; ZooScan: $p<0.01$) than oceanic stations (see also Table 1), consistent with the shelf stations being more productive (Fig. 10). On the other hand, the flatter slopes (LOPC: $p<0.01$; ZooScan: $p<0.01$) at the oceanic stations are

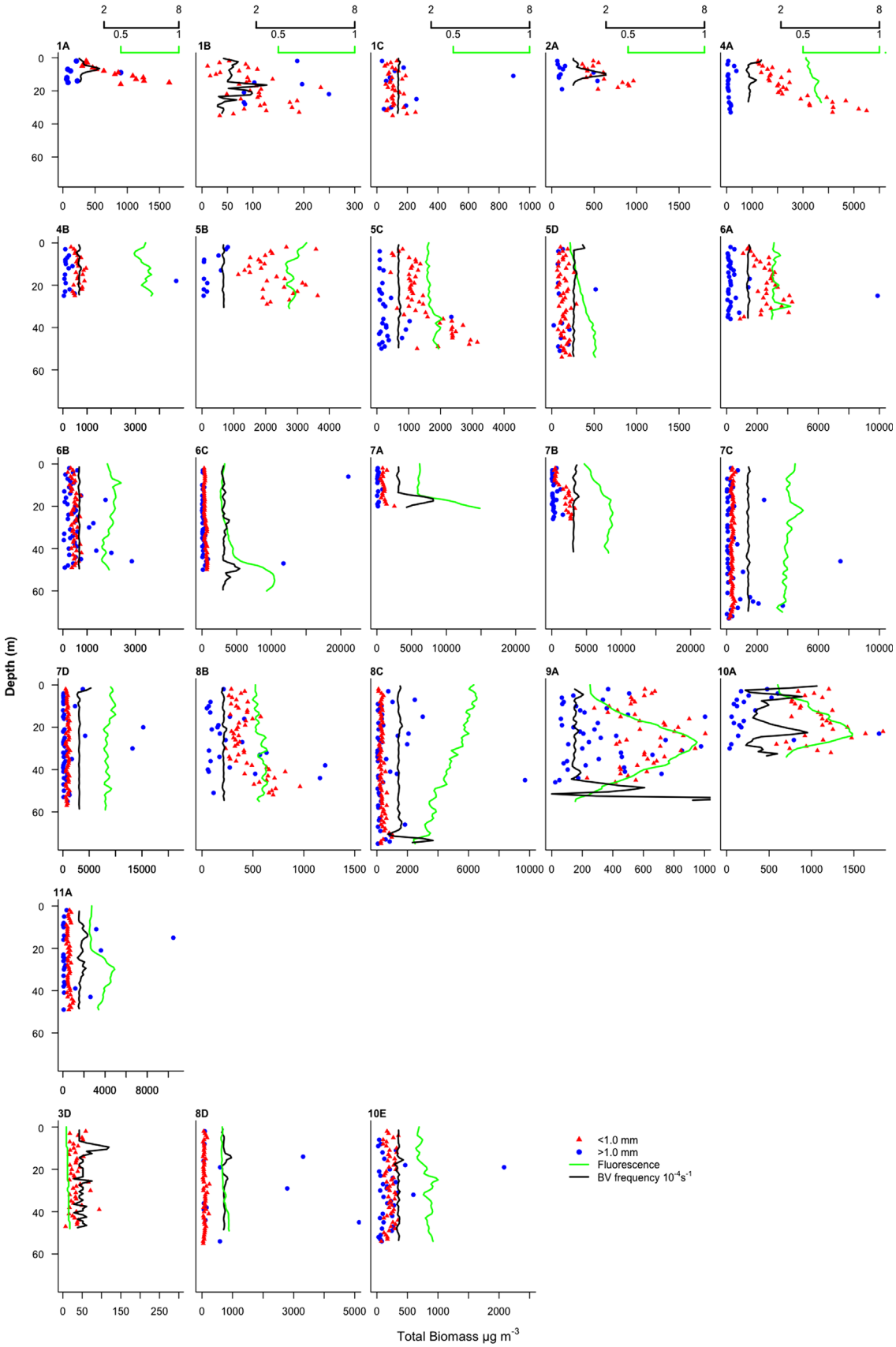

Fig. 5. Vertical profiles of particles <1 mm and >1 mm over the shelf. Last row represents stations above seamounts, despite their low depth ranges these were classified as oceanic stations since they are far from the coast. Black and green lines represent BV frequency $10^{-4}\,s^{-1}$ and chlorophyll fluorescence distributions, respectively (black and green axes on top). (For interpretation of the references to color in this figure legend, the reader is referred to the web version of this article.)

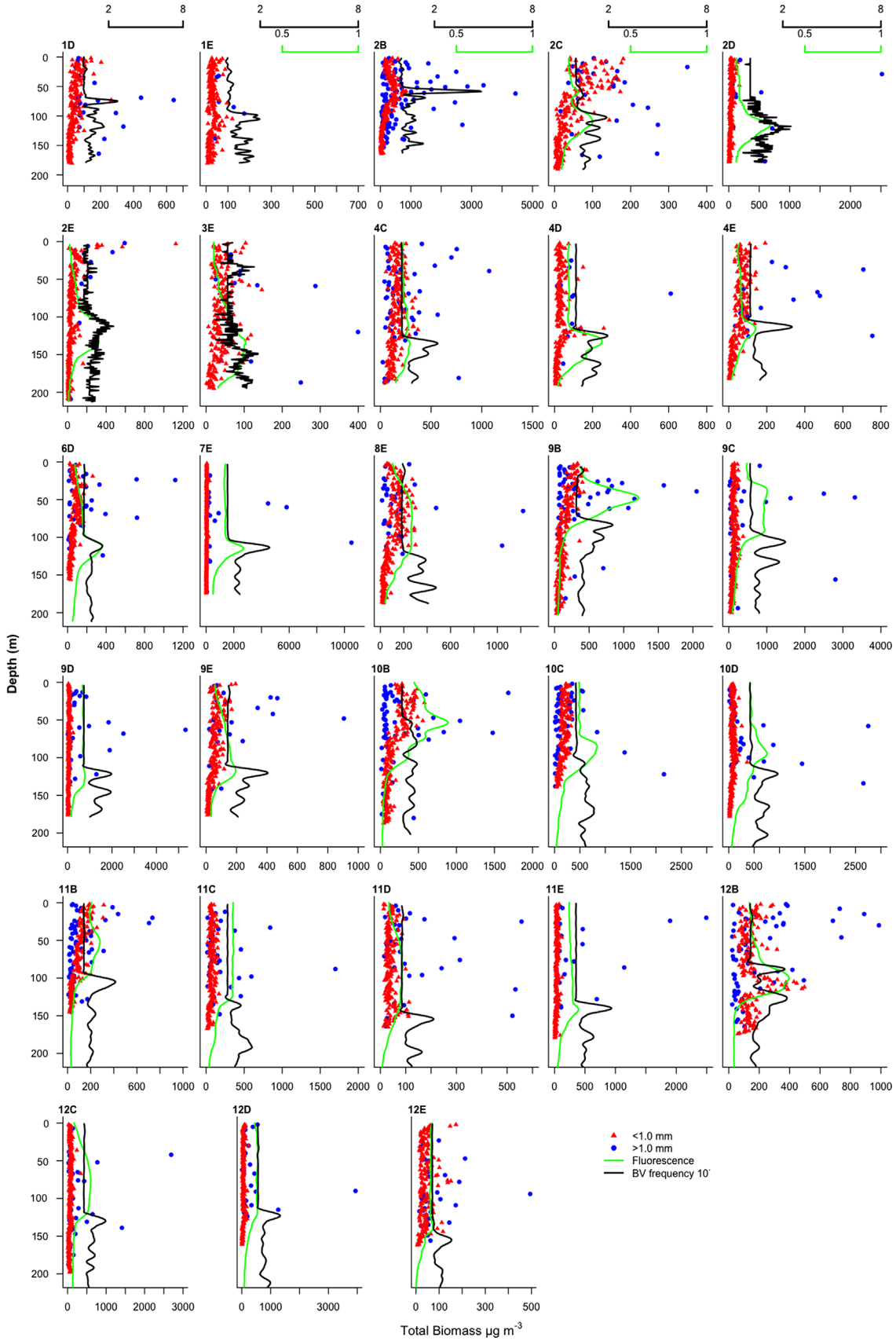

Fig. 6. Vertical profiles of particles <1 mm and >1 mm at the ocenic stations. For seamounts see Fig. 5. Black and green lines represent BV frequency $10^{-4}\,s^{-1}$ and chlorophyll fluorescence distributions, respectively (black and green axes on top). (For interpretation of the references to color in this figure legend, the reader is referred to the web version of this article.)

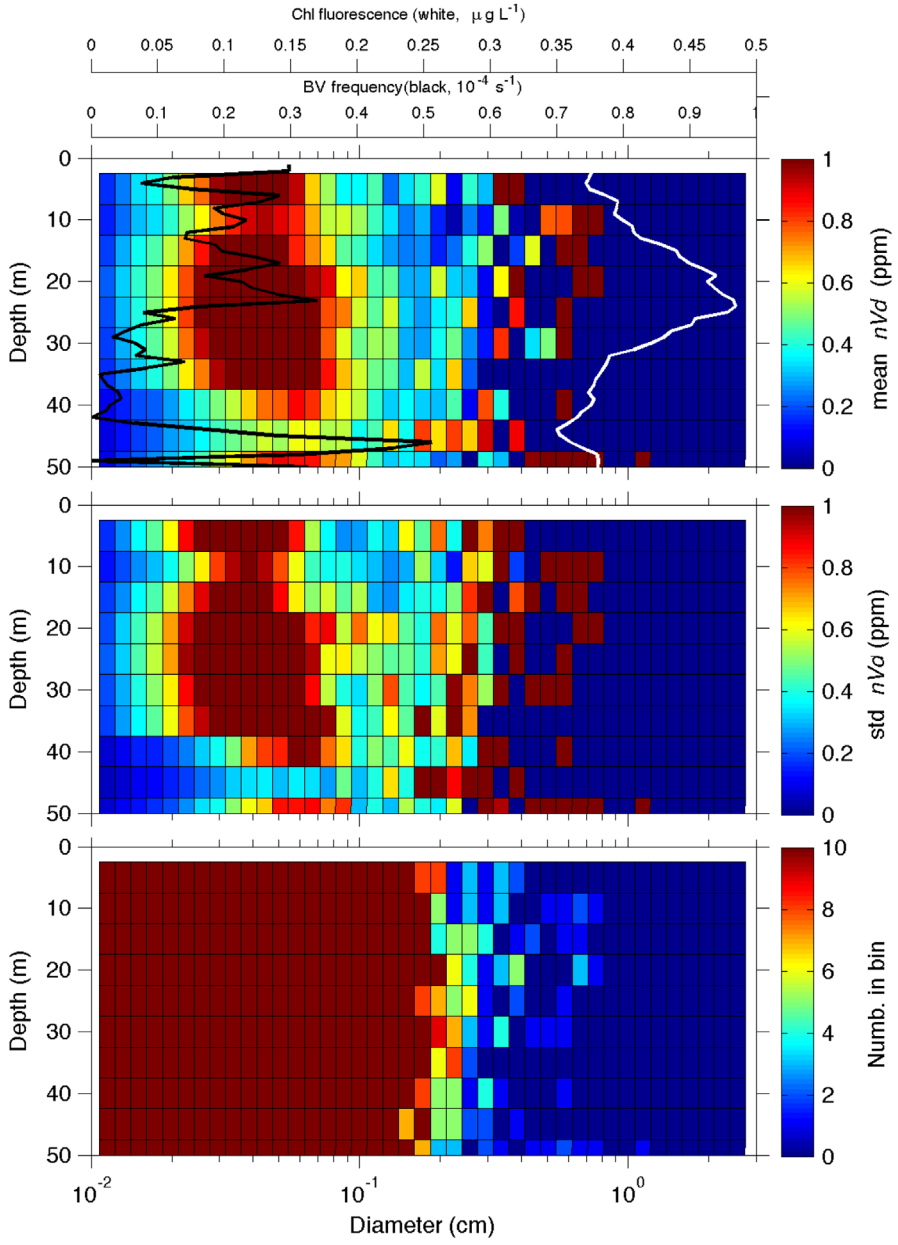

Fig. 7. Shelf station distribution of the particle normalized volume spectra (*nVds*) calculated from the LOPC observations; average (top panel) and standard deviation (middle panel) of *nVd*, as well as number of particles in each size range (bottom panel), are shown. The black line in the top panel indicates the average Brunt–Väisälä frequency; the white line indicates the average chlorophyll fluorescence. Size ranges shown as having 10 particles in lower panel actually have 10 or more. There is greater statistical confidence in concentrations calculated using larger numbers.

consistent with a greater contribution by larger organisms relative to small mesozooplankton.

The decrease in biomass for organisms smaller than 450 μm and resulting dome shape of the NBSS estimated by the ZooScan (Fig. 11) is consistent with the lower sampling efficiency of the 200 μm-mesh net at the smaller sizes. The higher NBSS intercepts calculated for the LOPC data could result from the sampling of additional particles, *i.e.* marine snow, a result of the inability of the LOPC to distinguish between living and non-living objects, as well as the tendency of nets to disrupt fragile detrital particles. Nevertheless, the higher biomass measured with the LOPC at the lower end of the size spectrum also results from the ability of the LOPC to detect small zooplankton down to size of 100 μm ESD (Herman et al., 2004), a size fraction that is generally sampled poorly by conventional nets but that can be a dominant component of zooplankton biomass (Hopcroft et al., 2001).

3.4. Mesozooplankton biomass size spectra

The size distributions of the major zooplankton taxa illustrate their contributions to the NBSS profile (Fig. 11). At the shelf stations, maxima of copepod and ostracod biomass size distributions were in phase with the NBSS peaks (around 0.5 mm); ostracods had another peak in a larger size class (around 0.85 mm). At the oceanic stations some groups, such as copepods, thaliaceans, and chaetognaths, had a broader size distribution without gaps in the upper end of the spectra. Therefore, the shallower slopes in the open ocean and steeper slopes over the shelf are the result of both lower abundance of the smaller and higher abundance of the larger organisms in the offshore stations and by differences in the ranges of size distribution for the main taxonomic groups.

Although the detritus size distribution is also superimposed with the NBSS on Fig. 11, it was not included in the NBSS

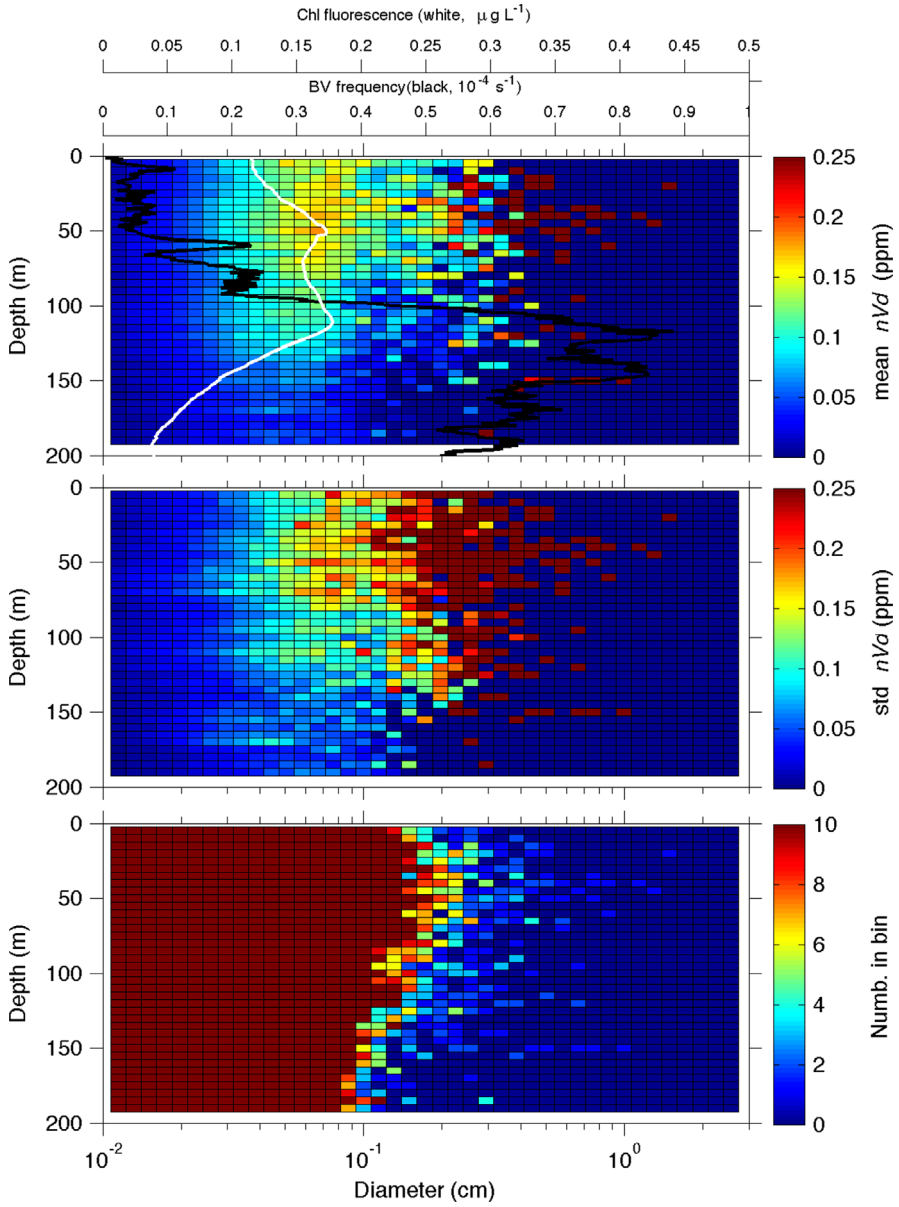

Fig. 8. Oceanic station distribution of the particle normalized volume spectra (*nVds*) calculated from the LOPC observations; *nVd* average (top panel) and standard deviations (middle panel), as well as number of particles in each bin (bottom panel), are shown. The black line in the top panel indicates the average Brunt–Väisälä frequency; the white line represents the average chlorophyll fluorescence. Size ranges shown as having 10 particles in lower panel actually have 10 or more.

calculations derived from ZooScan data (grey circles, Fig. 11) because detrital material is not properly collected by nets (González-Quirós and Checkley, 2006). However, we can make a spatial comparison assuming that the relative biases on detritus abundance estimates were the same in all samples. This results in shelf stations having almost one order of magnitude more detritus than the oceanic stations (Fig. 11).

4. Discussion

4.1. The regional spatial structure of particle distribution

The vertical structure of oceanographic properties was an important factor for the vertical distribution of small particles in the Abrolhos region, since <1 mm particles were more abundant in the mixed layer. The fluorescence peaks found within or above the pycnocline suggest the influence of thermohaline stratification on the phytoplankton distribution, consistent with the findings of Susini-Ribeiro et al. (2013). These associations between discontinuities in the water density, indicated by high values of the BV frequency, and the high concentrations of phytoplankton and sestonic particles have been reported often in other coastal and oceanic regions (*e.g.* Lampitt et al., 1993; MacIntyre et al., 1995; Sullivan et al., 2010), but remain virtually unstudied off tropical and subtropical SW Atlantic.

Despite the variability associated with the size distribution of particles in the Abrolhos Bank and vicinity, the average *nVd* distribution provided a general picture of the particle vertical structure at shelf and oceanic stations. The higher particle concentration on the shelf and higher contribution of larger particles to total biomass offshore are consistent with the steeper slopes and higher NBSS intercepts at the shelf relative to oceanic stations. The total particle volume decline contrasts with the increase in mesozooplankton biomass at the shelf stations toward the south, suggesting that there is a latitudinal gradient in the proportional

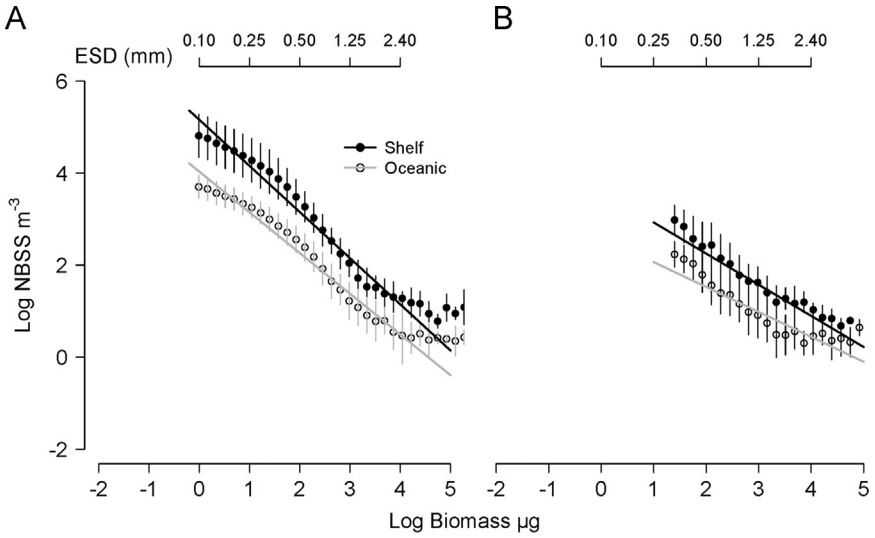

Fig. 9. Normalized Biomass Size Spectra (NBSS) estimated using the LOPC (A) and using preserved net samples analyzed with the ZooScan (B), for shelf and oceanic stations. Bottom axes show the particle biomasses, while top axes show the equivalent diameters.

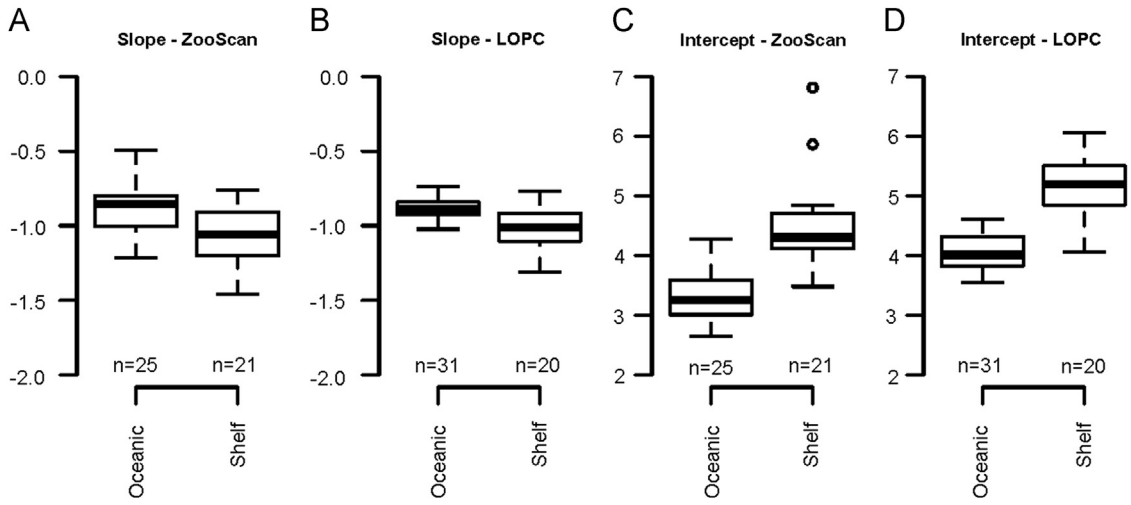

Fig. 10. Mean Normalized Biomass Size Spectra NBSS slopes ((A) and (B)) and intercepts ((C) and (D)) calculated using data from ZooScan ((A) and (C)) and LOPC ((B) and (D)) for shelf and oceanic stations. The Wilcoxon test detected significant differences between the two domains for all comparisons ($p < 0.05$).

distribution of living and non-living particles, with a higher detrital input over the bank than on the southern shelf, again consistent with the findings of Susini-Ribeiro et al. (2013). Although detrital abundance estimated by the ZooScan is not accurate in absolute numbers, it can provide additional useful information to compare shelf and oceanic stations. Because the LOPC samples include detritus, distributions calculated from LOPC data should have larger values for NBSS intercepts than those calculated using ZooScan data over the shelf, as has been observed in earlier analyses (Schultes and Lopes, 2009). Both, in the study of Schultes and Lopes (2009) and in the present analysis, the estimates from the two approaches were closer at oceanic stations, implying that most particles detected by the LOPC offshore were zooplankton (Figs. 8 and 9).

The Abrolhos Bank and the Vitória-Trindade Ridge form a topographical barrier to the Brazil Current (BC). In this region, eddies and cyclonic vortices, such as the Vitória Eddy (VE) (Schmid et al., 1995), develop along the eastern and southern shelf edges and promote upwelling or bottom intrusions of the cold and nutrient-rich South Atlantic Central Water (SACW). This water mass is known to increase phytoplankton production on the Brazilian shelf and is important as a natural eutrophication agent for the mixing layer (Saldanha-Corrêa and Gianesella, 2004). Gaeta et al. (1999) detected low nitrate concentration, chlorophyll biomass and primary productivity on the Abrolhos Bank and proposed that high pelagic productivity was restricted to the VE periphery. In our study, chlorophyll fluorescence and mesozooplankton biomass maxima had a more extensive distribution across the Abrolhos Bank and the southernmost shelf than they predicted and coincided with microphytoplankton spatial variations during the same cruise (Susini-Ribeiro et al., 2013).

Sediment resuspension and advection is effective on the inner shelf adjacent to the Caravelas estuarine system (Schettini et al., 2013), where the along-shelf momentum associated to wind and bottom stresses leads to strong north-northeastward currents in winter (Teixeira et al., 2013). This is probably the cause for the high total particle abundance recorded in the < 1 mm size range by the LOPC in station 4A, with no corresponding zooplankton peak.

Other forces should be associated with the development of the populations of larger organisms at the southernmost stations and offshore. For example, SACW seasonal intrusions in the southeast Brazil stimulate blooms of salps and higher contributions of larger organisms (Lopes et al., 1999; Resgalla et al., 2001). The offshore and southernmost areas are more likely to be influenced by SACW

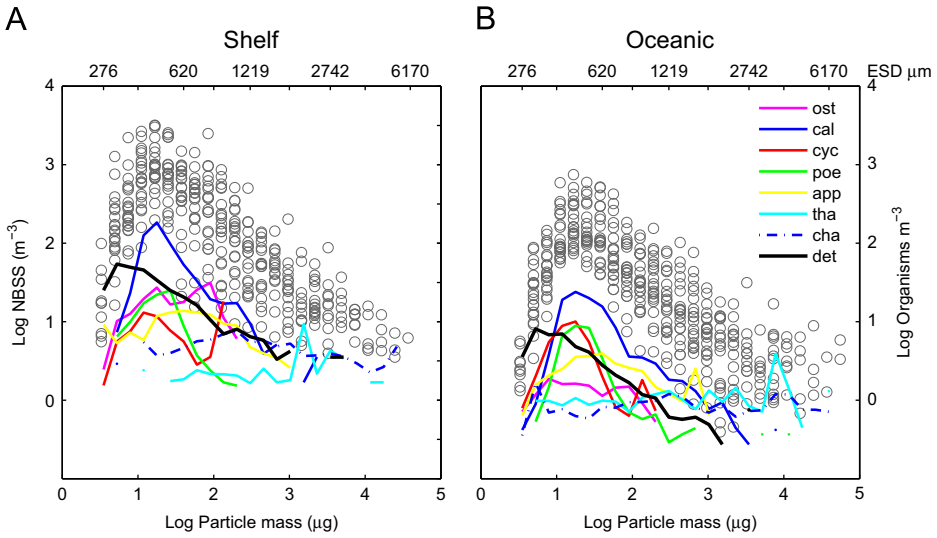

Fig. 11. Mesozooplankton Normalized Biomass Size Spectra (NBSS) superimposed on the average abundance size distributions (colored lines) of the main mesozooplankton taxa determined with the ZooScan (right axis). Shelf domain (A) and oceanic stations (B). Size distributions [equivalent spherical diameter (ESD), in mm] depicted on the upper axis. ost: *Ostracoda*; cal: *Calanoida*; cyc: *Cyclopoida*; poe: *Poecilostomatoida*; app: *Appendicularia*; tha: *Thaliacea*; cha: *Chaetognatha*; Det: Detritus. Bottom axes show the log of particle biomasses, while top axes show the equivalent diameters. (For interpretation of the references to color in this figure legend, the reader is referred to the web version of this article.)

in deeper depths, below the pycnocline, when bottom intrusions are induced by the BC interaction with the Abrolhos Bank topography and/or by the VE. Since the nutrients are provided in "pulses" during these intrusions, large phytoplankton has an advantage (Susini-Ribeiro et al., 2013) and populations of larger zooplankton are more likely to be developed, as we observed in the southern section of the study area, explaining the higher biomass of chaetognaths and thaliaceans (Fig. 4). We suggest that SACW bottom intrusions are triggering the population increase of these large organisms in the southern part of the Bank and in the southernmost oceanic stations.

4.2. Benthopelagic coupling

Benthopelagic coupling at the time of our study appeared to be strong. Benthic algal species and tychoplankton were an important component of the phytoplankton composition at the Abrolhos Bank stations (Susini-Ribeiro et al., 2013). Furthermore, crab larvae in the water column were all for reef-associated species (Koettker and Lopes, 2013). Although decapods biomass was usually $<5\%$ of total mesozooplankton biomass, our data set shows the importance of other benthic and demersal species for mesozooplankton biomass over Abrolhos Bank (Fig. 3C). Because of their larger average size, ostracods provided more biomass, with fewer numbers, to the pelagic system than in regions on the Abrolhos Bank where copepods dominated. The large number of ostracods in the plankton tows above the bank is probably from a bottom-dwelling species, which inhabit the bank region. Male ostracods produce bioluminescence as a display toward receptive bottom-dwelling females, and in specific habitats, such as in reef and seagrass systems, males synchronize in swarms after twilight (Morin, 1986). Most of the Abrolhos Bank stations with higher abundance of ostracods were sampled during the night ("moon" symbol in Fig. 3A), and many of those ostracods were carrying eggs (data not shown), suggesting that these peaks could have originated from a reproduction-driven behavior. Therefore, an important source of the pelagic biomass above the Abrolhos Bank must be provided by demersal species, further illustrating the importance of the reef system to the local pelagic productivity.

4.3. Size distributions and NBSS parameters

This is the first work to describe the vertical particle distribution and biomass size spectra in the Abrolhos Bank and vicinity, and one of the few to deal with mesozooplankton community structure in the area, examples of the latter being Valentin and Monteiro-Ribas (1993), Ekau (1999) and Knoppers et al. (1999). LOPC studies usually describe high latitude or temperate environments dominated by one or few large zooplankton species (Herman and Harvey, 2006; Zhou et al., 2009; Basedow et al., 2010; Basedow et al., 2013). At our low latitude sites, there were two domains: the continental shelf, including the area above the bank, and the oceanic blue waters. The shelf domain was dominated by small (<1 mm) calanoid copepods, which alternated in dominance with ostracods over the bank. High particle and plankton biomass and significantly steeper NBSS slopes indicated a relatively larger contribution of smaller particles to biomass.

In the oceanic domain, appendicularians and larger copepods, chaetognaths and salps were relatively more important, leading to flatter NBSS slopes. Cyclopoid copepods were also more abundant offshore than in the well-mixed waters of the Abrolhos inner shelf. Schultes et al. (2013) found that cyclopoids increased in abundance from coast to ocean along a transect on the Eastern Atlantic continental shelf, and suggested a better performance of the typical ambush-feeding behavior of cyclopoids (Saiz et al., 2003) in less turbulent, stratified offshore waters. In addition, cyclopoid copepods efficiently feed on small, flagellate phytoplankton species and microzooplankton, typical of the oligotrophic conditions in the oceanic domain (Paffenhoefer, 1998). Likewise, appendicularians are able to tap the nano- and picophytoplankton pool (Scheinberg et al., 2005) in oligotrophic waters.

Susini-Ribeiro (1999) has suggested a high degree of development of the microbial food web in the Abrolhos Bank area, with higher contribution of picoplankton relative to nano- and microplankton. She reported higher plankton biomass above the Abrolhos Bank and in the southern section of the continental shelf, and showed that phototrophic organisms dominated on the bank while heterotrophs were relatively more important in the open ocean. Analysis of microphytoplankton communities (Susini-Ribeiro et al., 2013) reported that large-celled species, particularly dinoflagellates and diatoms, occurred offshore as a response to

SACW intrusion. All their observations are in good agreement with our results for the size and taxonomic composition of mesozooplankton found in the study area.

Nutrient availability, as well as depth of the pycnocline, which influences turbulence and mixing intensity, appear to control the size and diversity of the microphytoplankton, which are the first links of the food web (Susini-Ribeiro et al., 2013). The assemblages of these organisms will reflect through the organisms developing in the chain. In our study, the higher NBSS intercepts at the shelf stations, including the Abrolhos Bank, imply high production within the smaller mesozooplankton size range and the steeper slopes suggest a less efficient biomass transfer to large size classes. The primary production is hence transferred to small calanoid copepods and, ultimately, to the benthic communities. The shallower NBSS slopes and lower intercepts at oceanic stations, in addition to their lower chlorophyll fluorescence, are consistent with a less productive system having higher energy transfer efficiency and biomass recycling (Zhou, 2006) and a larger number of trophic levels in the mesozooplankton and micronekton size range. These differences in the zooplankton size spectra between shelf and offshore areas can be explained as a consequence of different energy sources and food availability for the first elements of the food web.

4.4. NBSS theory applied

The association between the parameters of the linear regression fitted to the NBSS and the ecological features of planktonic systems (*e.g.* productivity, trophic structure) has been widely addressed in the literature. Sprules and Munawar (1986) in inland lakes and Iriarte and González (2004) off Chile found steeper NBSS slopes in oligotrophic systems compared to productive areas. They showed that in less productive systems a significant proportion of the primary productivity was provided by microbial food webs. These patterns should be a recurrent feature because small cells are favored in oligotrophic conditions due to their higher surface: volume ratio, which enables a more efficient nutrient assimilation. During upwelling events, larger cells have an advantage when turbulence is high and nutrients are available in pulses (Falkowski and Oliver, 2007). The consequence would be shallower slopes which indeed are observed in association with high production rates during upwelling events (Iriarte and González, 2004; San Martin et al., 2006).

On the other hand, Zhou et al. (2009) have argued that a high potential productivity is indicated by steeper slopes because of higher proportion of herbivorous zooplankton in the system (Zhou and Huntley, 1997; Zhou, 2006). Jennings and Warr (2003) studied the trophic structure of fish communities, and observed that low predator:prey body size ratios were characteristic of trophic webs with higher number of links. Jennings and Mackinson (2003) associated steeper NBSS slopes with those low ratios, which led them to suggest that such slopes indicate more stable environments. Hence, both shallower and steeper slopes have been considered as indicative of higher pelagic productivity, and steeper slopes have been associated with higher ecosystem stability. Therefore, we still need to be careful about using NBSS parameters as a proxy for system productivity or stability without previous information about the ecosystem. Different size ranges were used to calculate the NBSS for the above-mentioned studies (Table 2). For example, Zhou et al. (2009) estimated the NBSS for zooplankton $>250\,\mu m$ while Iriarte and González (2004) and San Martin et al. (2006) worked with a much smaller size spectra ($>1\,\mu m$), and Jennings and Mackinson (2003) investigated fish-sized biomass spectra.

We believe that integrated studies covering simultaneously a wide range of sizes and trophic levels are necessary to clarify whether NBSS-derived metrics and their interpretations are universally applicable to the aquatic ecosystem. This is a difficult task

Table 2
Comparison of mesozooplankton Normalized Biomass Size Spectra (NBSS) slopes and size ranges at different locations. Expanded from Matsuno et al. (2012).

Location/region	Unit	Size range (mm)	Slope	References
Chile—cold-nutrient-rich conditions	Carbon	0.7–210	−0.44	Iriarte and González (2004)
Gulf of St Lawrence (open water)	Biovolume	0.25–2	−0.47	Herman and Harvey (2006)
Barents Sea	Biovolume	0.25–14	−0.63	Basedow et al. (2010)
NW Mediterranean (protected area)	Wet weight	20–1200	−0.65	Macpherson et al. (2002)
Bay of Biscay (oceanic stations)	Carbon	0.27–1.7	−0.71 to −0.64	Sourisseau and Carlotti (2006)
Tasman Sea	Biovolume	0.11–3.3	−0.69	Baird et al. (2008)
Ushant Tidal Front (stratified side/offshore)	Carbon	0.5–5	−0.73	Schultes et al. (2013)
Chukchi Sea (less productive)	Biovolume	0.25–5	−0.86	Matsuno et al. (2012)
Gulf of St Lawrence (estuary)	Biovolume	0.25–2	−0.90	Herman and Harvey (2006)
Western Antarctic Peninsula (Fall)	Biovolume	0.25–14	−0.92	Zhou et al. (2009)
Chile—El Niño, oligotrophic conditions	Carbon	0.7–210	−0.93	Iriarte and González (2004)
Coral Sea	Biovolume	0.11–3.3	−0.97	Baird et al. (2008)
Southwest Coral Sea	Wet mass	0.25–2.5	−1.00	Suthers et al. (2006)
Bay of Biscay (coastal stations)	Carbon	0.27–1.7	−1.05 to −0.91	Sourisseau and Carlotti (2006)
NW Mediterranean (unprotected area)	Wet weight	20–1200	−1.04	Macpherson et al. (2002)
Scotia Sea (spring)	Carbon	Small phyto to large schyphomedusae	−1.09	Tarling et al. (2012)
North Iberian Shelf	Carbon	0.25–17	−1.11	Nogueira et al. (2004)
Chukchi Sea (more productive)	Biovolume	0.25–5	−1.11	Matsuno et al. (2012)
North Pacific Ocean	Carbon	0.18–4.0	−1.13	Rodriguez and Mullin (1986)
Northwest Atlantic Ocean	Carbon	0.07–8.0	−1.14	Quinones et al. (2003)
Ushant Tidal Front (front)	Carbon	0.5–5	−1.15	Schultes et al. (2013)
California Current	Carbon	0.2–3.3	−1.43	Huntley et al. (1995)
Ushant Tidal Front (mixed side/nearshore)	Carbon	0.5–5	−1.76	Schultes et al. (2013)
Western Antarctic Peninsula (Summer)	Biovolume	0.25–14	−1.80	Zhou et al. (2009)
Australian Estuary	Wet mass	0.25–1.6	−1.89	Moore and Suthers (2006)
California Bight	Biovolume	0.025–4.0	−2.30	Napp et al. (1993)
Brazilian Continental Shelf	Biovolume—ZooScan	0.25–8	−1.01	This study
(Coastal Stations and Abrolhos Bank)	Biovolume—LOPC	0.1–5	−1.25	This study
Brazilian Continental Shelf (Oceanic Stations)	Biovolume—ZooScan	0.25–8	−0.91	This study
	Biovolume—LOPC	0.1–5	−0.86	This study

as many methodological challenges are involved, such as that sampling efficiency must remain close to 100% across size groups and trophic levels to avoid unrealistic domes and gaps along the size spectra, and must adequately depict the variable spatial and temporal scales in life cycle strategies from bacteria to fish. This is still beyond our existing observational capabilities, but recent developments in automated systems for ocean biology studies (Karlson and Lopes, 2009; Stemmann and Boss, 2012) indicate that such approach is not that far in the horizon.

5. Conclusions

This study provided data on plankton and particle size spectra distribution and composition for an extensive shelf and oceanic area off Eastern Brazil (16–22°S) during winter conditions. Vertical profiles with an optical particle counter followed by image analysis of preserved net samples showed that the pelagic trophic structure in the area is influenced by water column stratification in the offshore domain, and by changes in water circulation in response to the complex seabed topography on the wide continental shelf of Abrolhos Bank.

An important finding of this study was the observation of high particle and plankton biomass associated with steep slopes and high intercepts of the Normalized Biomass Size Spectrum (NBSS) over the bank. Because estuarine influence on the Abrolhos coral reef ecosystem was minimal during the course of our observations (Schettini et al., 2013; Koettker and Lopes, 2013), the increased pelagic productivity and suspended particle concentration over the bank probably resulted from intense bentho-pelagic coupling. Low particle biomass, shallow slopes and low intercepts were found in the vertically stratified oceanic domain influenced by nutrient-rich waters below the mixed layer. These results, in combination with the significant contribution of large organisms to total biomass, mainly in the southernmost stations influenced by eddies and bottom intrusions, indicate high energy transfer efficiencies through the oceanic plankton food web. In addition, the relationship between water density stratification and particle abundance was apparent, as both small- (<1 mm) and large-sized (>1 mm) organisms were concentrated within or above the pycnocline in offshore areas.

Both LOPC and ZooScan were useful tools to provide rapid information on plankton size distribution and NBSS parameters. Although the instruments have different size detection limits and deal with different sampling efficiencies in the lower and upper ends of the size spectra, both detected similar patterns, including the significant differences in the NBSS slopes and intercepts between shelf and oceanic stations. Further studies with combined use of both instruments, as well as with additional sensors and platforms, can help to enhance our mechanistic understanding of the dynamics and ecological role of plankton and seston in aquatic environments.

Acknowledgments

We would like to thank the contributions from both anonymous reviewers, who helped us to improve the quality of this paper in many ways. David Checkley provided important insights during an early phase of manuscript preparation. CRM was supported by National Council for Scientific and Technological Development (CNPq), PhD scholarship grant 141409/2010-0 and 141793/2012-0. SS was supported by São Paulo Research Foundation (FAPESP), postdoctoral fellowship grant 06/06683-9. GAJ was supported by U. S. National Science Foundation (NSF) grant OCE03-52127. RML was supported by CNPq grant 307928/2010-1. The study was part of the project PROABROLHOS (CNPq grant 420219/2005-6 to Eurico Cabral de Oliveira).

References

Amado-Filho, G.M., Moura, R.L., Bastos, A.C., Salgado, L.T., Sumida, P.Y., Guth, A.Z., Francini-Filho, R.B., Pereira-Filho, G.H., Abrantes, D.P., Brasileiro, P.S., Bahia, R.G., Leal, R.N., Kaufman, L., Kleypas, J.A, Farina, M., Thompson, F.L., 2012. Rhodolith beds are major $CaCO_3$ bio-factories in the tropical South West Atlantic. PLoS One 7, e35171.

Baird, M.E., Timko, P.G., Middleton, J.H., Mullaney, T.J., Cox, D.R., Suthers, I.M., 2008. Biological properties across the Tasman Front off southeast Australia. Deep Sea Research Part I: Oceanographic Research Papers 55, 1438–1455.

Basedow, S.L., Tande, K.S., Zhou, M., 2010. Biovolume spectrum theories applied: spatial patterns of trophic levels within a mesozooplankton community at the polar front. Journal of Plankton Research 32, 1105–1119.

Basedow, S.L., Tande, K.S., Norrbin, M.F., Kristiansen, S.A., 2013. Capturing quantitative zooplankton information in the sea: performance test of laser optical plankton counter and video plankton recorder in a *Calanus finmarchicus* dominated summer situation. Progress in Oceanography 108, 72–80.

Benfield, M.C., Grosjean, P., Culverhouse, P.F., Irigoien, X., Sieracki, M.E., Lopez-Urrutia, A., Dam, H.G., Hu, Q., Davis, C.S., Hansen, A., Pilskaln, C.H., Riseman, E.M., Schultz, H., Utgoff, P.E., Gorsky, G., 2007. RAPID: Research on Automated Plankton Identification. Oceanography 20 (2), 172–187.

Blanchard, J.L., Jennings, S., Law, R., Castle, M.D., McCloghrie, P., Rochet, M.-J., Benoît, E., 2009. How does abundance scale with body size in coupled size-structured food webs? Journal of Animal Ecology 78, 270–280.

Boyd, P.W., Trull, T.W., 2007. Understanding the export of biogenic particles in oceanic waters: is there consensus? Progress in Oceanography 72, 276–312.

Brandini, F.P., Lopes, R., Gutseit, K.S., Spach, H.L., Sassi, R., 1997. Planctonologia na plataforma continental brasileira. Diagnose e Revisão Bibliográfica. Ministério do Meio Ambiente e da Amazônia Legal—IBAMA, FEMAR, Rio de Janeiro.

Checkley, D.M., Davis, R.E., Herman, A.W., Jackson, G.A., Beanlands, B., Regier, L.A., 2008. Assessing plankton and other particles *in situ* with the SOLOPC. Limnology and Oceanography 53, 2123–2136.

Costa, P.A.S., Braga, A., da, C., Rocha, L.O.F., 2003. Reef fisheries in Porto Seguro, eastern Brazilian coast. Fisheries Research 60, 577–583.

Ekau, W., 1999. Topographical and hydrographical impacts on zooplankton community structure in the Abrolhos Bank region, East Brazil. Archive of Fishery and Marine Research 47, 307–320.

Falkowski, P.G., Oliver, M.J., 2007. Mix and match: how climate selects phytoplankton. Nature Reviews Microbiology 5, 813–819.

Ferrier-Pagès, C., Witting, J., Tambutté, E., Sebens, K.P., 2003. Effect of natural zooplankton feeding on the tissue and skeletal growth of the scleractinian coral *Stylophora pistillata*. Coral Reefs 22, 229–240.

Finlay, K., Beisner, B.E., Patoine, A., Pinel-Alloul, B., 2007. Regional ecosystem variability drives the relative importance of bottom-up and top-down factors for zooplankton size spectra. Canadian Journal of Fisheries and Aquatic Sciences 64, 516–529.

Gaeta, S.A., Lorenzetti, J.A., Miranda, L.B., Susini-Ribeiro, S.M.M., Pompeu, M., Araujo, C.E.S., 1999. The Victoria Eddy and its relation to the phytoplankton biomass and primary productivity during the austral fall of 1995. Archive of Fishery and Marine Research 47, 253–270.

Gilabert, J., 2001. Short-term variability of the planktonic size structure in a Mediterranean coastal lagoon. Journal of Plankton Research 23, 219–226.

González-Quirós, R., Checkley, D.M., 2006. Occurrence of fragile particles inferred from optical plankton counters used *in situ* and to analyze net samples collected simultaneously. Journal of Geophysical Research 111, 1–12.

Giraudoux, P., 2012. Pgirmess: Data Analysis in Ecology. R Package Version 1.5.6. ⟨http:/CRAN.R-project.org/package=pgirmess⟩.

Gorsky, G., Ohman, M.D., Picheral, M., Gasparini, S., Stemmann, L., Romagnan, J.-B., Cawood, A., Pesant, S., Garcia-Comas, C., Prejger, F., 2010. Digital zooplankton image analysis using the ZooScan integrated system. Journal of Plankton Research 32, 285–303.

Graham, N.A.J., Dulvy, N.K., Jennings, S., Polunin, N.V.C., 2005. Size-spectra as indicators of the effects of fishing on coral reef fish assemblages. Coral Reefs 24, 118–124.

Grosjean, P., Picheral, M., Warembourg, C., Gorsky, G., 2004. Enumeration, measurement, and identification of net zooplankton samples using the ZOOSCAN digital imaging system. ICES Journal of Marine Science 61, 518–525.

Guidi, L., Jackson, G.A., Stemmann, L., Miquel, J.C., Picheral, M., Gorsky, G., 2008. Relationship between particle size distribution and flux in the mesopelagic zone. Deep Sea Research Part I: Oceanographic Research Papers 55, 1364–1374.

Herman, A.W., Beanlands, B., Phillips, E.F., 2004. The next generation of Optical Plankton Counter: The Laser-OPC. Journal of Plankton Research 26, 1135–1145.

Herman, A.W., Harvey, M., 2006. Application of normalized biomass size spectra to laser optical plankton counter net intercomparisons of zooplankton distributions. Journal of Geophysical Research 111, 1–9.

Hopcroft, R.R., Roff, J.C., Chavez, F.P., 2001. Size paradigms in copepod communities: a re-examination. Hydrobiologia 453/454, 133–141.

Huntley, M.E., Zhou, M., Nordhausen, W., 1995. Mesoscale distribution of zooplankton in the California Current in late spring, observed by optical plankton counter. Journal of Marine Research 53, 647–674.

Iriarte, J.L., González, H.E., 2004. Phytoplankton size structure during and after the 1997/98 El Niño in a coastal upwelling area of the northern Humboldt Current System. Marine Ecology Progress Series 269, 83–90.

Jackson, G.A., Checkley, D.M., 2011. Particle size distributions in the upper 100 m water column and their implications for animal feeding in the plankton. Deep Sea Research Part I: Oceanographic Research Papers 58, 283–297.
Jennings, S., Mackinson, S., 2003. Abundance-body mass relationships in size-structured food webs. Ecology Letters 6, 971–974.
Jennings, S., Warr, K.J., 2003. Smaller predator–prey body size ratios in longer food chains. Proceedings of the Royal Society B: Biological Sciences 270, 1413–1417.
Karlson, B., Lopes, R.M. (Orgs.), 2009. Observational Approaches to Community Structure, from Microbes to Zooplankton. Group Report, Workshop on Ocean Biology Observatories, SCOR, Venice, Sept. 2009. Available at: ⟨http:/www.scor-int.org/OBO2009/Microbes_and_Zooplankton_Report.pdf⟩.
Kerr, S.R., Dickie, L.M., 2001. The Biomass Spectrum: A Predator–Prey Theory of Aquatic Production. Columbia University Press, New York.
Knoppers, B., Meyerhöfer, M., Marone, E., Dutz, J., Lopes, R., Leipe, T., Camargo, R., 1999. Compartments of the pelagic system and material exchange at the Abrolhos Bank coral reefs, Brazil. Archive of Fishery and Marine Research 47, 285–306.
Koettker, A.G., Lopes, R.M., 2013. Meroplankton Spatial Structure and Variability on Abrolhos Bank and Adjacent Areas, with Emphasis on Brachyuran Larvae. Continental Shelf Research 70, 97–108.
Krupica, K.L., Sprules, W.G., Herman, A.W., 2012. The utility of body size indices derived from optical plankton counter data for the characterization of marine zooplankton assemblages. Continental Shelf Research 36, 29–40.
Lampitt, R.S., Wishner, K.F., Turley, C.M., Angel, M.V., 1993. Marine snow studies in the Northeast Atlantic Ocean: distribution, composition and role as a food source for migrating plankton. Marine Biology 116, 689–702.
Leão, Z.M.A.N., 1996. The coral reefs of Bahia: morphology, distribution and the major environmental impacts. Anais da Academia Brasileira de Ciências 68, 439–452.
Lopes, R.M., Brandini, F.P., Gaeta, S.A., 1999. Distribution patterns of epipelagic copepods off Rio de Janeiro (SE Brazil) in summer 1991/1992 and winter 1992. Hydrobiologia 411, 161–174.
MacIntyre, S., Alldredge, A.L., Gotschalk, C.C., 1995. Accumulation of marine snow at density discontinuities in the water column. Limnology and Oceanography 40, 449–468.
Macpherson, E., Gordoa, A., Garcıa-Rubies, A., 2002. Biomass size spectra in littoral fishes in protected and unprotected areas in the NW Mediterranean. Estuarine, Coastal and Shelf Science 55, 777–788.
Matsuno, K., Yamaguchi, A, Imai, I., 2012. Biomass size spectra of mesozooplankton in the Chukchi Sea during the summers of 1991/1992 and 2007/2008: an analysis using optical plankton counter data. ICES Journal of Marine Science 69, 1205–1217.
Moore, S.K., Suthers, I.M., 2006. Evaluation and correction of subresolved particles by the optical plankton counter in three Australian estuaries with pristine to highly modified catchments. Journal of Geophysical Research 111, 1–14.
Morgan, P.P., 1994. SEAWATER: A library of MATLAB Computational Routines for the Properties of Sea Water.
Morin, J.G., 1986. “Firefleas” of the sea: luminescent signaling in marine ostracode crustaceans. Insect Behavioral Ecology 69, 105–121.
Napp, J.M., Ortner, P.B., Pieper, R.E., Holliday, D.V., 1993. Biovolume-size spectra of epipelagic zooplankton using a Multi-frequency Acoustic Profiling System (MAPS). Deep Sea Research Part I: Oceanographic Research Papers 40, 445–459.
Nogueira, E., González-Nuevo, G., Bode, A., Varela, M., Morán, X.A.G., Valdés, L., 2004. Comparison of biomass and size spectra derived from optical plankton counter data and net samples: application to the assessment of mesoplankton distribution along the northwest and North Iberian Shelf. ICES Journal of Marine Science 61, 508–517.
Paffenhoefer, G.-A., 1998. On the relation of structure, perception and activity in marine planktonic copepods. Journal of Marine Systems 15, 457–473.
Porter, J.W., 1976. Autotrophy, heterotrophy, and resource partitioning in Caribbean reef-building corals. The American Naturalist 110, 731–742.
Quinones, R.A., 1994. A comment on the use of allometry in the study of pelagic ecosystem processes. Scientia Marina 58, 11–16.
Quinones, R.A., Platt, T., Rodriguez, J., 2003. Patterns of biomass size spectra from oligotrophic waters of the northwest Atlantic. Progress in Oceanography 57, 405–427.
R Development Core Team 2011. R: A Language and Environment for Statistical Computing. R Foundation for Statistical Computing, Vienna, Austria. ISBN 3-900051-07-0, ⟨http:/www.R-project.org/⟩.
Resgalla, JR, De La Rocha, C., Montú, M., C., 2001. The influence of Ekman transport on zooplankton biomass variability off southern Brazil. Journal of Plankton Research 23 (6), 641–650.
Rodriguez, J., Mullin, M.M., 1986. Relation between biomass and body weight of plankton in a steady state oceanic ecosystem. Limnology and Oceanography 31, 361–370.
Russell, B.C., 1983. The food and feeding habits of rocky reef fish of north-Eastern New Zealand. New Zealand Journal of Marine and Freshwater Research 17, 121–145.
Saiz, E., Calbet, A., Broglio, E., 2003. Effects of small-scale turbulence on copepods: the case of *Oithona davisae*. Limnology and Oceanography 48, 1304–1311.
Saldanha-Corrêa, F.M.P., Gianesella, S.M.F., 2004. A microcosm approach on the potential effects of the vertical mixing of water masses over the primary productivity and phytoplankton biomass in the southern Brazilian coastal region. Brazilian Journal of Oceanography 52, 167–182.
San Martin, E., Harris, R.P., Irigoien, X., 2006. Latitudinal variation in plankton size spectra in the Atlantic Ocean. Deep Sea Research Part II: Topical Studies in Oceanography 53, 1560–1572.
Sarkar, D., 2008. Lattice: Multivariate Data Visualization with R. Springer, New York. (ISBN 978-0-387-75968-5).
Schettini, C.A.F., Pereira, M.D., Siegle, E., Miranda, L.B., Silva, M.P., 2013. Residual fluxes of suspended sediment in a tidally dominated tropical estuary. Continental Shelf Research. (Available online 20 March 2013).
Scheinberg, R.D., Landry, M.R., Calbet., A., 2005. Grazing of two common appendicularians on the natural prey assemblage of a tropical coastal ecosystem. Marine Ecology Progress Series 294, 201–212.
Schmid, C., Schafer, H., Podestá, G., Zenk, W., 1995. The Vitória Eddy and its relation to the Brazil Current. Journal of Physical Oceanography 25, 2532–2546.
Schultes, S., Lopes, R.M., 2009. Laser Optical Plankton Counter and ZooScan intercomparison in tropical and subtropical marine ecosystems. Limnology and Oceanography: Methods 7, 771–784.
Schultes, S., Sourisseau, M., Le Masson, E., Lunven, M., Marié, L., 2013. Influence of physical forcing on mesozooplankton communities at the Ushant tidal front. Journal of Marine Systems 109–110 (supplement), S191–S202.
Sheldon, R.W., Prakash, A., Sutcliffe, J., 1972. The size distribution of particles in the ocean. Limnology and Oceanography 17, 327–340.
Sourisseau, M., Carlotti, F., 2006. Spatial distribution of zooplankton size spectra on the French continental shelf of the Bay of Biscay during spring 2000 and 2001. Journal of Geophysical Research 111, 1–12.
Sprules, W.G., Munawar, M., 1986. Plankton size spectra in relation to ecosystem productivity, size, and perturbation. Canadian Journal of Fisheries and Aquatic Sciences 436, 1789–1794.
Stemmann, L., Boss, E., 2012. Plankton and particle size and packaging: from determining optical properties to driving the biological pump. Annual Review of Marine Science 4 (1), 263–290.
Stock, C., Powell, T., Levin, S., 2008. Bottom-up and top-down forcing in a simple size-structured plankton dynamics model. Journal of Marine Systems 74, 134–152.
Soutelino, R.G., Gangopadhyay, A., Silveira, I.C.A., The Roles of Vertical Shear and Topography on the Eddy Formation Near the Site of Origin of the Brazil Current 2013.
Sullivan, J.M., Donaghay, P.L., Rines, J.E.B., 2010. Coastal thin layer dynamics: Consequences to biology and optics. Continental Shelf Research 30, 50–65.
Susini-Ribeiro, S.M.M., 1999. Biomass distribution of pico-, nano- and microplankton on the continental shelf of Abrolhos, East Brazil. Archive of Fishery and Marine Research 47, 271–284.
Susini-Ribeiro, S.M.M., Pompeu, M., Gaeta, S.A., Souza, J.S.D., Masuda, L.S.D., Topographical and Hydrographical Impacts on the Structure of Microphytoplankton Assemblages on the Abrolhos Bank Region, Brazil 2013.
Suthers, I.M., Taggart, C.T., Rissik, D., Baird, M.E., 2006. Day and night ichthyoplankton assemblages and zooplankton biomass size spectrum in a deep ocean island wake. Marine Ecology Progress Series 322, 225–238.
Tarling, G.A., Stowasser, G., Ward, P., Poulton, A.J., Zhou, M., Venables, H.J., McGill, R.A.R., Murphy, E.J., 2012. Seasonal trophic structure of the Scotia Sea pelagic ecosystem considered through biomass spectra and stable isotope analysis. Deep Sea Research Part II: Topical Studies in Oceanography 59–60, 222–236.
Teixeira, C.E.P, Lessa, G.C., Cirano, M., Lentini, C.A., The Inner Shelf Circulation on the Abrolhos Bank, 18oS, Brazil 2013.
Valentin, J.L., Wanda, M., Monteiro-Ribas, W.M., 1993. Zooplankton community structure on the east-southeast Brazilian continental shelf (18–23°S latitude). Continental Shelf Research 13, 407–424.
Warnes, G.R. Includes R Source Code and/or Documentation Contributed by Ben Bolker and Thomas Lumley, 2013. Gtools: Various R Programming Tools. R Package Version 2.7.1. ⟨http:/CRAN.R-project.org/package=gtools⟩.
Werner, T.B., Pinto, L.P., Dutra, G.F., Pereira, P.G.P., 2000. Abrolhos 2000: conserving the Southern Atlantic's richest coastal biodiversity into the next century. Coastal Management 28, 99–108.
Zhou, M., 2006. What determines the slope of a plankton biomass spectrum? Journal of Plankton Research 28, 437–448.
Zhou, M., Huntley, M.E., 1997. Population dynamics theory of plankton based on biomass spectra. Marine Ecology Progress Series 159, 61–73.
Zhou, M., Tande, K.S., Zhu, Y., Basedow, S., 2009. Productivity, trophic levels and size spectra of zooplankton in northern Norwegian shelf regions. Deep Sea Research Part II: Topical Studies in Oceanography 56, 1934–1944.